Chemical Abundances in Gaseous Nebulae
AAA Workshop Series 12, 2016
G. Hägele, M. Cardaci & E. Pérez-Montero, eds.

arXiv:1701.05435v1 [astro-ph.GA] 19 Jan 2017

Invited Review

Spatially resolved properties for extremely metal-poor star-forming galaxies with Wolf-Rayet features and high-ionization lines

C.Kehrig[1]

[1]*Instituto de Astrofísica de Andalucía, CSIC, Apartado de correos 3004, E-18080 Granada, Spain*

Abstract.
Extremely metal-poor, high-ionizing starbursts in the local Universe provide unique laboratories for exploring in detail the physics of high-redshift systems. Also, their ongoing star-formation and haphazard morphology make them outstanding proxies for primordial galaxies. Using integral field spectroscopy, we spatially resolved the ISM properties and massive stars of two first-class low metallicity galaxies with Wolf-Rayet features and nebular HeII emission: Mrk178 and IZw18. In this review, we summarize our main results for these two objects.

1. Introduction

Local extremely metal-poor [i.e., 12+log (O/H) $\leq$ 7.7][1] starburt galaxies are among the least chemically evolved objects in the nearby Universe, and are considered to be analogues to the first star-forming (SF) systems (e.g. Izotov et al. 1994, 2009; Hunter & Hoffman 1999; Kehrig et al. 2006; Sanchez Almeida et al. 2016). Studying these metal-deficient starbursts is needed to learn more about the evolution and feedback from massive stars [e.g. Wolf-Rayet (WR) stars] in high-z galaxies, and for exploring in detail the physics of the farway Universe.
The presence of WR signatures (most commonly a broad feature centered at $\sim$ 4680 Å or "blue bump") in the spectra of some metal-poor SF galaxies [e.g. Legrand et al. 1997; Guseva, Izotov & Thuan 2000; Cairós et al. 2010; Kehrig et al. 2016 (hereafter K16)] challenges current single star (rotating/non-rotating) stellar evolution models that fail in reproducing the WR content in low metallicity (Z) environments (see Brinchmann, Kunth, & Durret 2008 and references therein; Leitherer et al. 2014). Thus, investigating the WR content and radiative feedback from WR stars (WRs) in metal-poor starbursts is crucial to test the models at low metallicity. The study on formation and thereabouts of gamma-ray bursts and Type Ib/c SN progenitors, believed to be WRs in metal-poor galaxies, may also benefit from the investigation presented here (e.g. Woosley & Bloom 2006)

[1]The precise value of the metallicity defining extremely metal-poor galaxies varies in the literature (see Guseva et al. 2016 and references therein)

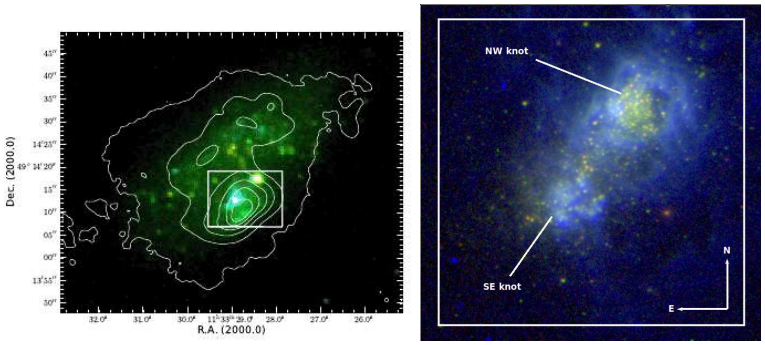

Figure 1. *Left panel*: Colour-composite SDSS image of Mrk178 overlaid with the observed FOV of WHT/INTEGRAL ($\sim$ 16"×12") represented by the white box. *Right panel*: Colour-composite HST image of IZw18. The observed FOV of PMAS (16"×16") is represented by the white box.

The spectra of SF galaxies are dominated by strong nebular emission lines which are mainly formed via the photoionization by hot massive stars. High-ionization lines, like HeII, are often seen in the spectra of low metallicity SF galaxies at both low and high redshift [e.g. Kehrig et al. 2004; Thuan & Izotov 2005; Shirazi & Brinchmann 2012; Cassata et al. 2013; Kehrig et al. 2013, 2015 (hereafter K13, K15)]. The expected harder spectral energy distribution (SED) and higher nebular gas temperatures at low metallicities should boost the supply of hard ionizing photons. While the presence of hard radiation is well established in some nearby metal-deficient SF galaxies, the origin of this radiation is much less clear, in spite of several attempts to account for it (e.g. Thuan & Izotov 2005; K15). Overall, several mechanisms for producing hard ionizing radiation have been proposed, such as WR stars, primordial zero-metallicity stars, high-mass X-ray binaries and fast radiative shocks. However, no mechanism has emerged clearly as the leading candidate. Reconsidering the underlying assumptions in the analysis of high-ionization nebular emission in metal-poor galaxies is key to advance our understanding of their properties.

We have used integral field spectroscopy (IFS) to obtain a more believable view of extremely metal-poor, high-ionizing starbursts in the local Universe (see Fig.1; K13, K15, K16). IFS has many advantages in comparison with long-slit spectroscopy (e.g. Cairós et al. 2009; James et al. 2011; Kehrig et al. 2012; Pérez-Montero et al. 2013; Duarte Puertas et al. 2016). IFS allows a more precise spatial correlation between massive stars and nebular properties through a 2D analysis. IFS is a powerful technique to probe and solve issues related with aperture effects too. Long-slit observations may fail in detecting WR features due to their faintness with respect to the stellar continuum emission and spatial distribution of WR stars across the galaxy. In particular in low-Z objects, the dilution of WR features and the difficulty in spectroscopically identifying WR stars is even stronger owing to the steeper Z dependence of WR star winds which lowers the line luminosities of such stars (e.g. Crowther & Hadfield 2006). Kehrig et al. (2008) demonstrated for the first time the power of IFS in minimizing the

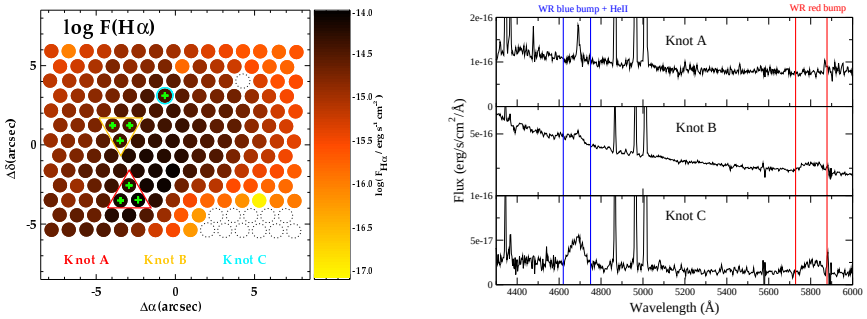

Figure 2. *Left panel*: Map of Hα emission line. The diameter of each spaxel is $\sim$ 1" ($\sim$ 20 pc, our resolution element size). The three WR knots (A, B and C) are labelled on the Hα flux map, and the spaxels where we detect WR features are marked with green crosses. *Right panel*: Integrated spectrum for the 3 knots in which WR features are detected. The spectral range for both blue and red WR bumps are marked (see K13).

WR bump dilution and finding WR stars in extragalactic systems where they were not detected before (see also Cairós et al. 2010; James et al. 2011).
Here, we summarize the main results from the analysis of our new integral field unit (IFU) data of two extremely metal-poor, high-ionizing SF galaxies: Mrk178, *the closest metal-poor WR galaxy* (see K13), and IZw18, *the most metal-deficient HeII-emitting SF galaxy known in the local Universe* (see K15, K16).

2. Results

2.1. Mrk178: the closest metal-poor WR galaxy

In K13 we present the first optical IFS study of Mrk 178 based on IFU data obtained with the INTEGRAL IFU at the 4.2m WHT, Roque de los Muchachos observatory (see Fig.1). The proximity of Mrk 178 (distance $\sim$ 3.9 Mpc) combined with the IFS technique allow us to locate and resolve SF knots hosting a few WRs, and also to characterize the WR content. In addition, we are able to probe the spatial correlation between massive stars and the properties of the surrounding ISM.
We defined three WR knots from which two (knots A and C) are identified for the first time in K13. The WR knot spectra reveal the presence of nitrogen-type and carbon-type WR stars in Mrk 178 (see Fig.2). By comparing the observed spectra of the WR knots with SMC/LMC template WRs, we empirically estimate a lower limit for the number of WRs ($\geq$ 20) in our Mrk178 FOV that is already higher than that currently found in the literature ($\sim$ 2-3 WRs from Guseva et al. 2000). Regarding the ISM properties, our statistical analysis suggests that spatial variations in the gaseous T_e[OIII] exist and that the scatter in T_e[OIII] can be larger than that in O/H within the observed FOV. Thus, caution should be exercised when analysing integrated spectra of SF systems which do not necessarily represent the "local" ISM properties around massive

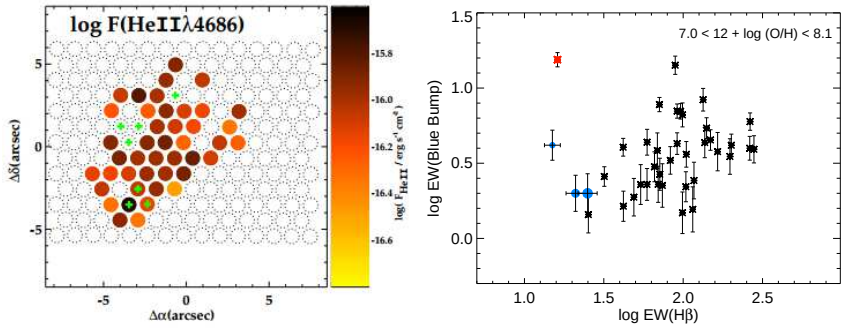

Figure 3. *Left panel*: map of nebular HeIIλ4686 line; spaxels where we detect WR features are marked with green crosses. *Right panel*: EW(WR blue bump) vs. EW(Hβ). Asterisks show values from SDSS DR7 for metal-poor WR galaxies; the red one represents Mrk178. The three blue circles, from the smallest to the biggest one, represent the 5", 7" and 10" diameter apertures from our IFU data centered at the SDSS fiber of Mrk178 (see K13 for details).

star clusters. The nebular chemical abundance in Mrk 178 is homogeneous over spatial scales of hundreds of parsecs. The representative metallicity of Mrk 178 derived is 12+log(O/H) = 7.72 $\pm$ 0.01 (error-weighted mean value of O/H and its corresponding statistical error). To probe the presence of small-scale ($\sim$ 20 pc) localized chemical variations, we performed a close inspection of the chemical abundances for the WR knots from which we find a possible localized N and He enrichment, spatially correlated with WR knot C (see also James et al. 2011).
Nebular HeIIλ4686 emission is shown to be spatially extended reaching well beyond the location of the WRs (see HeIIλ4686 map in Fig.3). Shock ionization and X-ray binaries are unlikely to be significant ionizing mechanisms since Mrk178 is not detected in X-rays, and measured values of [SII]/Hα ($<$ 0.20) are lower than the typical ones observed in SNRs. The main excitation source of HeII in Mrk178 is still unknown.
From SDSS spectra of metal-poor WR galaxies, we found a too high EW(WR bump)/EW(Hβ) value for Mrk178, which is the most deviant point in the sample (see Fig.3). Using our IFU data, we showed that this curious behaviour is caused by aperture effects, which actually affect, to some degree, the EW(WR bump) measurements for all galaxies in left panel of Fig.3. Also, we demonstrated that using too large an aperture, the chance of detecting WR features decreases. This result indicates that WR galaxy samples constructed on single fibre/long-slit spectrum basis may be biased in the sense that WR signatures can escape detection depending on the distance of the object and on the aperture size.

2.2. IZw18: the most metal-deficient HeII-emitting SF galaxy in the nearby Universe

We performed new IFS observations of IZw18 using the PMAS IFU on the 3.5m telescope at CAHA (see K15, K16). IZw18 is a high-ionization galaxy which

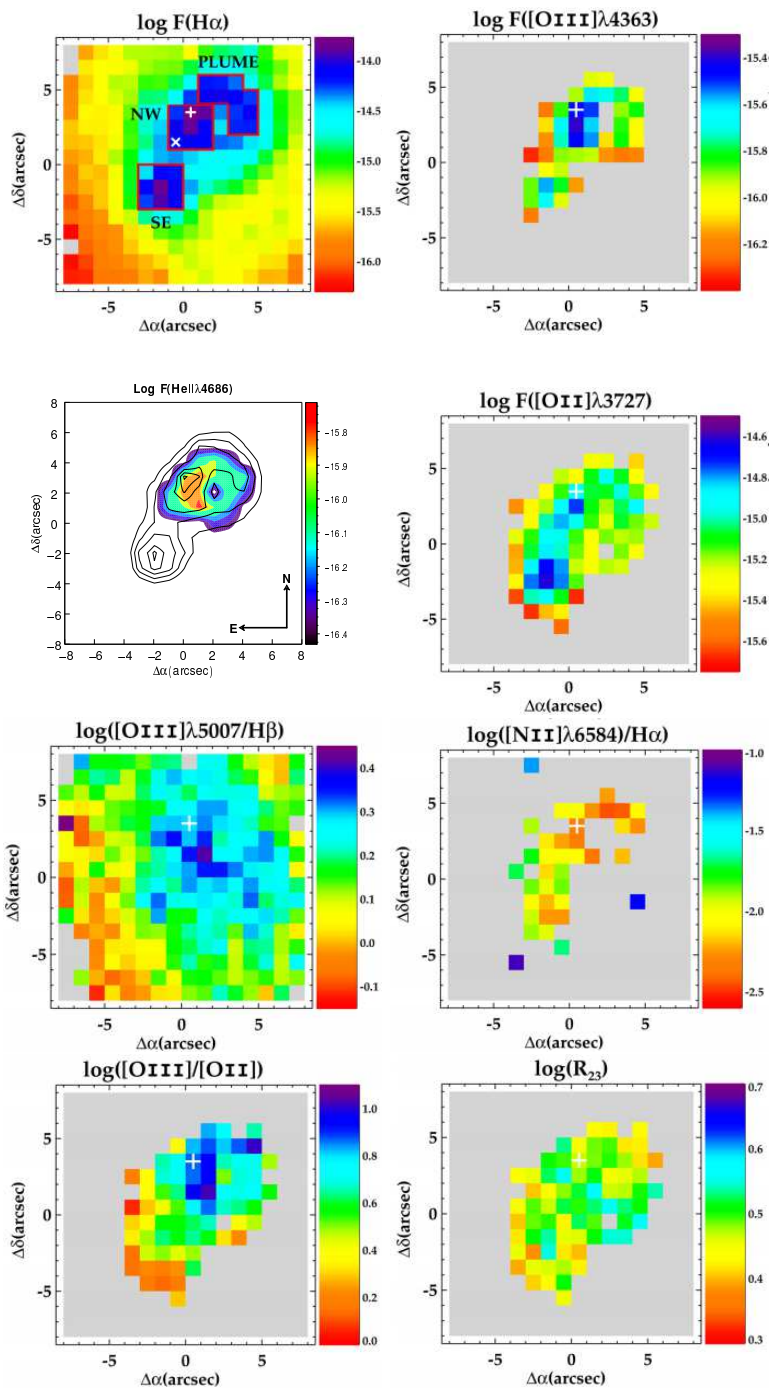

Figure 4. Emssion line flux and line ratio maps: Hα, [OIII]λ4363, HeIIλ4686, [OII]λ3727, [OIII]λ5007/Hβ, [NII]λ6584/Hα, [OIII]/[OII], R_{23}. Spaxels with no measurements available are left grey. Each spaxel corresponds to 1" ($\sim$ 88 pc at the distance of 18.2 Mpc). The peak of Hα emission is marked with a plus (+) sign on all maps. The cross on the Hα map marks the spaxel where we detect the WR feature (see K16). The Hα map also shows the boundaries of the areas that we use to create the 1D spectra of the NW and SE knots, and of the "plume" region (see K16 for details). The HeII map is presented as color-filled contour plot and isocontours of the Hα emission line are shown overplotted for reference (see K15).

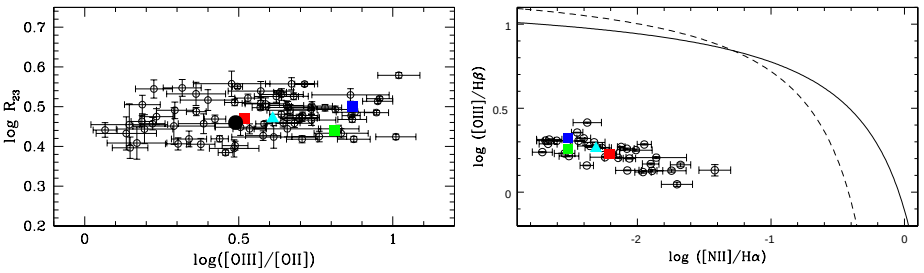

Figure 5. *Left panel*: The relation between log(R_{23}) and log([OIII]/[OII]). Open circles correspond to individual spaxels from the data cube. *Right panel*: The "BPT" diagnostic diagram, showing [OIII]λ5007/Hβ vs. [NII]λ6584/Hα. The [SII]/Hα-BPT and [OI]/Hα-BPT are shown in K16. Blue, red, and green squares are the line ratios measured from the 1D spectra of the NW knot, SE knot and "plume", respectively; the cyan triangle shows the line ratio values from the total integrated spectrum of IZw18; the black circle corresponds to the line ratios from the spectrum of the "halo" of IZw18 (see K16 for details)

is among the most metal-poor (Z$\sim$ 1/40 $Z_{\odot}$; e.g. Pagel et al. 1992; Vílchez & Iglesias-Páramo 1998) starbursts in the local Universe. This makes IZw18 an excellent analog for primeval systems. Our IFU aperture samples the entire IZw18 main body and an extended region of its ionized gas (see Fig.1); the two main SF regions of IZw18 are usually referred to as the north-west (NW) and southeast (SE) components. We have created and analysed maps for relevant emission lines, line ratios and physical-chemical properties of the ionized gas.
Fig.4 reveals that the spatial distribution of the emission in Hα, HeIIλ4686 and [OIII]λ4363 is peaked towards the NW component while the [OII]λ3727 emission reaches its maximum at the SE component. Also, by inspecting the maps of [OIII]λ5007/Hβ, [NII]λ6584/Hα and [OIII]/[OII], there is a clear tendency for the gas excitation to be higher at the location of the NW knot and thereabouts. The spatial distribution of the abundance indicator R_{23} is found to be relatively flat without any significant peak (see the R_{23} map in Fig.4). However, the ionization parameter diagnostic [OIII]/[OII] does not show a homogeneous distribution with the highest values of [OIII]/[OII] found within the NW knot, as mentioned above. Our spaxel-by-spaxel analysis shows that there is no dependence between R_{23} and the ionization parameter across IZw18 (see right panel in Fig.5). Other examples of SF regions whith large range of excitation and constant metallicity can be found in the literature (e.g. Pérez-Montero et al. 2011; K13).
Over $\sim$ 0.30 kpc^2, using the [OIII]λ4363 line flux, we compute T_e[OIII] values between $\sim$ 15,000-25,000 K (see Figs.6 & 7); it is the first time that T_e[OIII] $>$ 22,000 K are derived for IZw18. Fig.7 shows that the highest values of T_e[OIII] are not an effect of an overestimation during the measurement of the [OIII]λ4363 flux. If we look at the "BPT" diagram (Fig.5), we see that all spaxels occupy the SF region, indicating that shocks do not play an important role in the gas excitation in IZw18. Thus, the enhanced T_e[OIII] values derived are expected to be associated primarily with photoionization from hot massive stars, and

T_e[OIII] errors due to shocks should be negligible. We note that more than 70% of the higher-T_e[OIII] (> 22,000 K) spaxels are HeIIλ4686-emitting spaxels too. This reinforces the existence of a harder ionizing radiation field towards the NW SF knot.

Our statistical analysis shows an important degree of nonhomogeneity for the T_e[OIII] distribution and that the scatter in T_e[OIII] can be larger than that in O/H within the observed [OIII] λ4363-emitting region. We find no statistically significant variations in O/H (derived directly from T_e[OIII]) across the PMAS-IFU aperture, indicating a global homogeneity of the O/H in IZw18 over spatial scales of hundreds of parsecs. The representative metallicity of IZw18 derived here, from individual spaxel measurements, is 12 + log(O/H) = 7.11 $\pm$ 0.01 (error-weighted mean value of O/H and its corresponding statistical error). The prevalence of a substantial degree of homogeneity in O/H over IZw18 can constrain its chemical history, suggesting an overall enrichment phase previous to the current burst.

We took advantage of our IFU data to create 1D integrated spectra for regions of interest in the galaxy. For the first time, we derive the IZw18 integrated spectrum by summing the spaxels over the whole FOV. Physical-chemical properties of the ionized gas were derived from these selected region spectra. We also show that the derivation of O/H and N/O does not depend on the aperture size used. This is a relevant result for studies of high-redshift SF objects for which only the integrated spectra are available.

PopIII-star siblings: a possible culprit behind the extended nebular HeIIλ4686 emission in IZw18

Narrow HeII emission in SF galaxies has been suggested to be mainly associated with photoionization from WRs, but WRs cannot satisfactorily explain the HeII-ionization in all cases, particularly at lowest metallicities where nebular HeII emission is often seen and observed to be stronger (e.g. Kehrig et al. 2004; Shirazi & Brinchmann 2012; James et al. 2016). Why is studying the formation of HeII emission relevant ? HeII emission indicates the presence of high energy photons (E $\geq$ 54 eV), and so provides essential constraints on the SEDs of hot massive stars. HeII-emitters are apparently more frequent among high-z galaxies than for local objects (Kehrig et al. 2011; Cassata et al. 2013). Actually, narrow HeII emission has been claimed to be a good tracer of PopIII-stars (the first very hot metal-free stars) in distant galaxies (e.g. Schaerer 2003); these stars are believed to have contributed significantly to the reionization of the Universe, a challenging subject in contemporary cosmology. In fact, searching for PopIII-hosting galaxy candidates is among the main science drivers for next generation telescopes (e.g., JWST; E-ELT). However, we should note that the origin of narrow HeII lines remains difficult to understand in many nearby and distant SF galaxies/regions (e.g., Kehrig et al. 2011; Shirazi & Brinchmann 2012; Gräfener & Vink 2015; Pallottini et al. 2015; Hartwig et al. 2016). One of the main reasons why we do not fully understand the physics behind the formation of nebular HeII is the lack of direct probes on HeII-ionizing hot stars. Detailed investigation of the HeII emission at low redshift is needed to better interpret distant narrow HeII-emitters and therefore gaining a deeper understanding of the reionization epoch. IZw18, as the most metal-poor HeII-emitter in the local Universe, is an ideal object to perform this study.

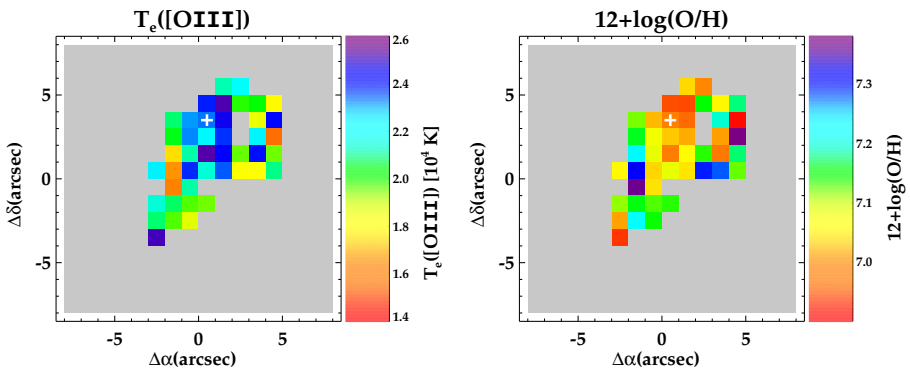

Figure 6. *Left panel*: Map of T_e[OIII] derived directly from the measurement of the [OIII]λ4363 flux above 3σ detection limit. *Right panel*: Map of O/H derived from T_e[OIII].

Our IFS data reveal for the first time the entire nebular HeIIλ4686-emitting region (see map of HeIIλ4686 in Fig.4) and corresponding total HeII-ionizing photon flux [$Q(HeII)_{obs}$] in IZw18. These observations combined with stellar model predictions point out that conventional excitation sources (e.g., single WRs, shocks, X-ray binaries) cannot convincingly explain the total $Q(HeII)_{obs}$ derived for IZw18 (see K15 for details). Other mechanisms are probably also at work. If the HeII-ionization in IZw18 is due to stellar sources, these might be peculiar very hot stars. Based on models of very massive O stars (Kudritzki 2002), $\sim$ 10-20 stars with 300 $M_\odot$ at Z_{IZw18} [or lower, down to Z$\sim$(1/100) $Z_\odot$] can reproduce our total $Q(HeII)_{obs}$ (see also Szécsi et al. 2015). However, the super-massive star scenario requires a cluster mass much higher than the mass of the IZw18 NW knot (where the HeII region is located), and it would not be hard enough to explain the highest HeII/Hβ values observed. On top of that, the existence of super-massive 300 $M_\odot$ stars remains heavily debated, and an extrapolation of the IMF predicting such massive stars remains unchecked up to now (Vink et al. 2014).

Considering that the previous scenarios fail in reproducing the observations, and that searches for PopIII-hosting galaxies have been carried out using HeII lines (e.g. Schaerer 2008; Cassata et al. 2013), we thought that (nearly) metal-free hot stars may hold the key to the HeII ionization in IZw18. To test this hypothesis, as an approximation of (nearly) metal-free stars in IZw18 – the so-called *PopIII-star siblings* – we compared our observations with current models for rotating Z=0 stars (Yoon et al. 2012), which in fact reproduce our data better: $\sim$8-10 of such stars with M_{ini}=150 $M_\odot$ can explain the total $Q(HeII)_{obs}$ and the highest HeII/Hβ values observed. The PopIII-star sibling scenario, invoked for the first time in IZw18 by K15, goes in line with the results by Lebouteiller et al. (2013). While gas in IZw 18 is very metal-deficient but not primordial, Lebouteiller et al. (2013) have pointed out that the HI envelope of IZw 18 near the NW knot contains essentially metal-free gas pockets. These gas pockets could provide the raw material for making such *PopIII-star siblings* (see also Tornatore et al. 2007).

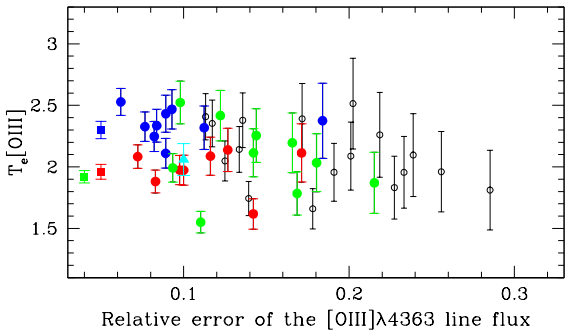

Figure 7. T_e[OIII] derived directly from the [OIII]λ4363 line vs. the relative error of the measurement. Open circles represent individual spaxels; blue, red and green circles indicate the individual spaxels used to create the 1D spectra of the NW knot, SE knot, and plume, respectively. Squares indicate the values measured from the 1D integrated spectra with the same colour-code as used for the individual spaxels.

3. Summary and Conclusions

A brief overview of the first optical IFU observations of two nearby, extremely metal-poor *bursty*-galaxies (Mrk178 and IZw18) is presented. Clues of the early-universe can be found in our cosmic backyard through this class of objects which are excellent primordial analogues, and are key in understanding galaxy evolution. IFS studies of such galaxies enable extended insight into their "realistic" ISM and massive stars, therefore providing constraints on high-redshift galaxy evolution, and on metal-poor stellar models. Our data provide useful testbench for realistic photoionization models at the lowest metallicity regime.
The elusive PopIII-hosting galaxies have been searched through the high-ionization HeII line signature. The HeII line is in comfortable reach of next generation telescopes, like JWST and TMT, which will detect the rest-frame UV of thousands of galaxies during the epoch of reionization. In light of these new observations, a more sophisticated understanding of the high-ionization phenomenon is required to interpret the data in a physically meaningful manner, and to possibly constrain sources responsible for the Universe reionization. Using IFU data, we were able to recover the *total* HeII luminosity and perform a *free-aperture* investigation on the formation of narrow HeII line. Our observations of IZw18 test the current poorly-constrained models for metal-poor massive stars, and suggest that peculiar hot stellar sources, as PopIII-star siblings, might be culprits for the HeII-ionization in this galaxy. This result emphasizes the need to identify extremely metal-poor HeII-emitting targets, such as IZw18, and the power of IFS for such kind of investigation.

Acknowledgments. CK gratefully acknowledges the co-authors and referees from K13, K15 and K16 who made significant contribution to the results presented in this review.

References

Brinchmann. J., Kunth D., Durret F., 2008, A&A, 485, 657
Cairós, L.M., et al. 2009, ApJ, 707, 1676
Cairós, L.M., et al. 2010, A&A, 520, A90
Cassata P., et al. 2013, A&A, 556, A68
Crowther P. A., Hadfield L. J., 2006, A&A, 449, 711
Duarte Puertas, S., et al. 2016, arXiv:1611.07935
Gräfener, G.; Vink, J. S., 2015, A&A, 578, L2
Guseva N. G., Izotov Y. I., Thuan T. X., 2000, ApJ, 531, 776
Guseva, N. G., Izotov, Y. I., Fricke, K. J., Henkel, C., 2016, arXiv:1611.06881
Hartwig, T., et al. 2016, MNRAS, 462, 2184
Hunter, D. A., Hoffman, L., 1999, AJ, 117, 2789
Izotov Y. I., Thuan T. X., Lipovetsky V. A., 1994, ApJ, 435, 647.
Izotov, Y. I., et al. 2009, A&A, 503, 61
James, B. L., et al. 2011, MNRAS, 430, 2097
James, B. L., et al. 2016, arXiv:1611.05888
Kehrig, C., Telles, E., Cuisinier, F., 2004, AJ, 128, 1141
Kehrig, C., Vílchez, Telles, E., et al. 2006,A&A, 457, 477
Kehrig, C., Vílchez, J. M., Sánchez, S. F., et al. 2008, A&A, 477, 813
Kehrig, C., Oey, M. S., Crowther, P. A., et al. 2011, A&A, 526, A128
Kehrig, C., et al. 2012, A&A, 540, A11
Kehrig, C., Pérez-Montero, E., Vílchez, J. M., et al. 2013, MNRAS, 432, 2731
Kehrig, C., Vílchez, J. M., Pérez-Montero, E., et al. 2015, ApJL, 801, L28
Kehrig, C., Vílchez, J. M., Pérez-Montero, E., et al. 2016, MNRAS, 459, 2992
Kudritzki R. P., 2002, ApJ, 577, 389
Lebouteiller V., Heap S., Hubeny I., Kunth D., 2013, A&A, 553, A16
Legrand, F., et al. 1997, A&A, 326, L17
Leitherer C., et al. 2014, ApJS, 212, 14
Pagel, B. E. J., et al. 1992, MNRAS, 255, 325
Pallottini, A., Ferrara, A., Pacucci, F., et al. 2015, MNRAS, 453, 2465
Pérez-Montero, E. et al., 2011, A&A, 532, A141
Pérez-Montero, E., Kehrig, C., Brinchmann, J., et al. 2013, Adv. Astron., 837392
Sanchez Almeida, J., et al. 2016, arXiv:1612.00273
Schaerer D., 2003, A&A, 397, 527
Schaerer, D., 2008, IAUSS, 255, 66
Shirazi M., Brinchmann J., 2012, MNRAS, 421, 1043
Szécsi, D., Langer, N., Yoon, S.-C., et al. 2015, A&A, 581, A15
Tornatore, L., Ferrara, A., Schneider, R., 2007, MNRAS, 382, 945
Thuan., T. X., Izotov, Y. I., 2005, ApJS, 161, 240
Vílchez J. M., Iglesias-Páramo J., 1998, ApJ, 508, 248
Vink, J. S., 2014, arXiv:1406.4836
Woosley, S. E., Bloom, J. S., 2006, ARA&A, 44, 507
Yoon S.-C., Dierks A., Langer N., 2012, A&A, 542, A113